 

https://doi.org/10.1070/QEL16300

# Laboratory reflectometer for the investigation of optical elements in a wavelength range of 5–50 nm: description and testing results

S.A. Garakhin, I.G. Zabrodin, S.E. Zuev, I.A. Kas'kov, A.Ya. Lopatin, A.N. Nechay, V.N. Polkovnikov, N.N. Salashchenko, N.N. Tsybin, N.I. Chkhalo, M.V. Svechnikov

*Abstract.* **We describe a laboratory reflectometer developed at the IPM RAS for precision measurements of spectral and angular dependences of the reflection and transmission coefficients of optical elements in a wavelength range of 5–50 nm. The radiation is monochromatised using a high-resolution Czerny–Turner spectrometer with a plane diffraction grating and two spherical collimating mirrors. A toroidal mirror focuses the probe monochromatic beam on a sample. The X-ray source is a highly ionised plasma produced in the interaction of a high-power laser beam with a solid target at an intensity of $10^{11}$–$10^{12}$ W cm$^{-2}$. To stabilise the emission characteristics, the target executes translatory and rotary motions in such a way that every pulse irradiates a new spot. The short-focus lens is protected from contamination by erosion products with the use of a specially designed electromagnetic system. The samples under study are mounted on a goniometer is accommodated in a dedicated chamber, which provides five degrees of freedom for samples up to 500 mm in diameter and two degrees of freedom for a detector. The sample mass may range up to 10 kg. The X-ray radiation is recorded with a detector composed of a CsI photocathode and two microchannel plates. A similar detector monitors the probe beam intensity. The spectral reflectometer resolution is equal to 0.030 nm with the use of ruled gratings with a density of 900 lines mm$^{-1}$ (spectral range: 5–20 nm) and to 0.067 nm for holographic gratings with a density of 400 lines mm$^{-1}$ (spectral range: 10–50 nm). We analyse the contribution of higher diffraction orders to the probe signal intensity and the ways of taking it into account in the measurements. Examples are given which serve to illustrate the reflectometer application to the study of multilayer mirrors and filters.**

***Keywords:*** *reflectometer, goniometer, soft X-ray radiation, extreme ultraviolet radiation, laser-produced plasma, multilayer mirror.*

## 1. Introduction

To improve the fabrication technology of X-ray optical elements requires measuring the X-ray optical data (the spectral, angular, and polarisation dependences of reflection and transmission coefficients, as well as the scattering diagrams) of the produced samples at the working wavelengths. This problem is solved in full measure in synchrotron radiation centres. However, researchers' affiliation with only the synchrotron sources severely limits their possibilities. In particular, the properties of thin films and nanostructures may undergo a strong change during transportation, while the development of experimental methods and technologies requires real-time information about the physical properties of a synthesised object. This problem manifested itself most clearly in the development of modern multilayer optics. Practice suggests that developing high-performance multilayer structures calls for the acquisition of on-line data about their properties, and so the trend of recent years involves the development of multifunctional laboratory reflectometers.

Today there are several approaches to the solution of this problem. The first approach, which was pursued by the physicists of our country (A.P. Lukirskii's school), consists in the development of Rowland-mount reflectometers with a spherical grazing-incidence diffraction grating and one immobile slit. Employed most often are RSM-500 spectrometers/monochromators [1, 2]. For a source of soft X-ray radiation use is made of a demountable X-ray tube attached to the mobile part of the spectrometer/monochromator. In this case, a goniometer chamber of virtually arbitrary size is accommodated behind the immobile exit slit. An example of this configuration is provided by the reflectometer [3] equipped with a goniometer providing five degrees of freedom for samples and two for a detector. The reflectometer permits studying X-ray optics of arbitrary surface shape up to 300 mm in diameter, with a numerical aperture of up to 0.5.

An advantage of this approach is its high spectral resolution, which is provided by the diffraction grating and is wavelength-independent throughout the working wavelength range. For instance, with the use of a diffraction grating with a radius of curvature of 6 m and a density of 600 lines mm$^{-1}$ the resolution is equal to 0.01 nm in a wavelength range from 0.6 to 5 nm [3]. An obvious disadvantage of this approach is that the existence of a mobile slit permits using only small-size and low-power X-ray radiation sources. High-quality measurements may actually be performed only with the characteristic lines of the anode materials of the X-ray tube.

An alternative approach implemented in Ref. [4] consists in the use of a spherical diffraction grating with immobile slits. Spectral scanning is carried out by simple grating rotation. For a source of X-ray radiation use is made of laser-produced plasmas. A cylindrical mirror mounted cross-wise to the grating is employed to reduce the astigmatism of the spherical grating, increase the collection angle for the source radiation, and focus the radiation in the vertical plane. At present there are several instruments of this type in the world, which fit out the leading centres involved in the research and

**S.A. Garakhin, I.G. Zabrodin, S.E. Zuev, I.A. Kas'kov, A.Ya. Lopatin, A.N. Nechay, V.N. Polkovnikov, N.N. Salashchenko, N.N. Tsybin, N.I. Chkhalo, M.V. Svechnikov** Institute for Physics of Microstructures, Russian Academy of Sciences, 7 ul. Akademicheskaya, 603087 Afonino, Kstovskii raion, Nizhnii Novgorod region, Russia;
e-mail: nechay@ipm.sci-nnov.ru, polkovnikov@ipm.sci-nnov.ru

Received 6 February 2017; revision received 9 March 2017
*Kvantovaya Elektronika* **47** (4) 385–392 (2017)
Translated by E.N. Ragozin

development in the area of modern X-ray optics (see, for instance, Ref. [5]).

The second alternative approach introduced in Ref. [6] involves the use of a varied line-space grating, which is illuminated by a converging beam produced by a focusing grazing-incidence mirror. One of the most remarkable implementations of this approach was reported in Ref. [7].

An advantage of the alternative approaches is a higher (by approximately two-three orders of magnitude) X-ray source power in comparison with the X-ray tube as well as the possibility of working with a continuous spectrum. The main disadvantage consists in the relatively narrow spectral range that maintains a high spectral resolution. In the case of spherical grating, this stems from the fact that the focusing condition of the Rowland circle is violated in the grating rotation. The use of plane varied line-space gratings provides a partial solution of this problem by expanding the high-resolution wavelength range to about an octave [6–8].

Modern X-ray optical tasks like the making of imaging multilayer reflective optics of diffraction-limited quality for next-generation lithography or for microscopy in the water and carbon transparency windows [9–11] call for a substantially higher resolution of the spectral instruments along with a smooth wavelength scanning, including the domain of anomalous dispersion of the optical constants of materials that make up the samples under investigation.

Here we propose a reflectometer developed at the IPM RAS, which combines a high spectral resolution typical for the instruments of the first type and a high-power source of continuum radiation used with the reflectometers of the second type. The reflectometer design and the underlying physical principles were described at length in Refs [12, 13]. In the present work we describe the instrument already completed and put into service. The emphasis is placed on the description of reflectometer's components and the results of testing its characteristics. We also give examples of its application to the study of multilayer mirrors, which serve to illustrate the capabilities of the instrument.

## 2. Optical configuration, elements and principle of operation of the reflectometer

Figure 1 depicts the optical reflectometer configuration, which was borrowed from Ref. [1]. The main elements of the instrument are a laser plasma pulsed source (LPPS) of soft X-ray (SXR) and extreme ultraviolet (EUV) radiation, a Czerny–Turner spectrometer/monochromator (CTSM), which provides the requisite level of monochromatisation and the geometric size of the probe beam at the sample under investigation, as well as a (5+2)-axis goniometer, which permits studying samples of arbitrary surface shape up to 500 mm in diameter.

In the development of an X-ray spectrometer/monochromator we adopted the Czerny–Turner configuration with two collimating mirrors and a plane diffraction grating. Unlike the traditionally used spectrometers/monochromators of the Rowland type, this configuration provides their characteristic high spectral resolution and a broad working range, but in doing this it leaves unchanged the positions of the entrance and exit slits. This almost entirely removes the limitations on the weight and size of the radiation source and reflectometer. It is precisely this property of the Czerny–Turner configuration that made it possible to go over from a low-power X-ray tube to a laser-plasma radiation source.

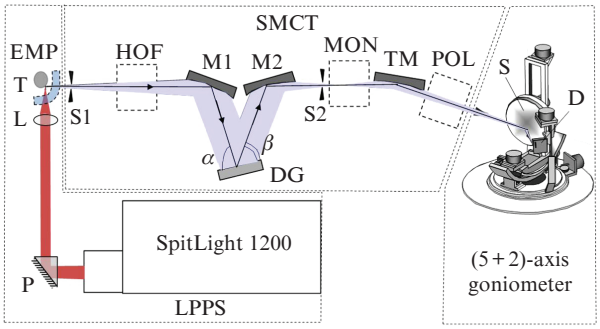


**Figure 1.** X-ray optical configuration of the reflectometer: (CTSM) Czerny–Turner spectrometer/monochromator; (LPPS) laser plasma pulsed X-ray source; (SpitLight 1200) Nd:YAG laser model; (P) deflecting prism; (L) focusing lens; (T) target; (EMP) electromagnetic protection from contamination; (S1, S2) entrance and exits spectrometer slits; (HOF) higher-order filter; (M1, M2) spherical collimating mirrors; (DG) plane diffraction grating; (TM) toroidal mirror; (MON) monitor of probe beam intensity; (POL) polariser; (S) sample under investigation; (D) detector.

An advantage of this kind of spectrometer/monochromator over the spectrometers that employ stationary slits and a plane varied line-space grating is a broader wavelength range in which a high spectral resolution is maintained.

The principle of instrument operation is as follows. The radiation of a SpitLight 1200 $Q$-switched Nd:YAG laser (working wavelengths, 532 and 1064 nm; pulse energy, 800 and 1200 mJ, respectively; pulse repetition rate, 10 Hz; pulse duration, 7 ns) is focused onto a target T to a spot approximately 100 μm in diameter (intensity: $\sim 10^{12}$ W cm$^{-2}$) with the use of a short-focus lens L. The radiation emanating from the plasma-produced plume is incident onto the entrance slit S1 of the spectrometer/monochromator. Mounted directly above the target is the electromagnetic protection (EMP) system, which prevents the entrance slit and the lens from being contaminated by the products of target erosion.

To stabilise the emission characteristics, by analogy with Ref. [5] the target (made of stainless steel, in our case) executes translatory and rotary motion in such a way that every laser pulse irradiates a new spot. This target design prevents the appearance of 'craters' on its surface, which remains relatively smooth even after several 'passes' of laser radiation over the target. The target smoothness leads to the constancy of irradiated surface area (the laser intensity in the focal spot is the critical parameter which defines the intensity and spectrum of plasma emission) and to the absence of screening of the radiation emitted by the plasma.

The entrance (S1) and exit (S2) slits are located at the meridional foci of the mirrors M1 and M2, respectively. Mirror M1 converts the divergent radiation beam emanating from the slit to a parallel beam, which is incident on a plane diffraction grating at an angle $\alpha$. The diffracted parallel monochromatic beams are incident on mirror M2 and focused in its focal plane. The beam diffracted at an angle $\beta$ is focused onto the exit slit S2.

The spectral scanning is effected by grating rotation in accordance with the diffraction grating equation

$$\cos\alpha - \cos\beta = m\lambda/D, \qquad (1)$$

where $m$ is the order of diffraction; $\lambda$ is the wavelength; $D$ is the grating period; $\alpha$ and $\beta$ are the angles of incidence and

diffraction, respectively. A special feature of this wavelength scanning scheme is that the sum of angles

$$\Phi = \alpha + \beta \tag{2}$$

remains constant irrespective of the wavelength. This condition signifies that the angular and linear dispersion of the spectrometer are hardly changed throughout the scanning range. This is easily seen by differentiating relation (1) with respect to the angle of diffraction and making, in view of the smallness of the angles, the substitution $\sin\alpha \simeq \alpha$:

$$\frac{\mathrm{d}\lambda}{\mathrm{d}\beta} \simeq \frac{D}{m}(\alpha + \beta) = \frac{D}{m}\Phi. \tag{3}$$

The spectral range is determined by the grating period and the working angles. The longest wavelength $\lambda_{\max}$ is achieved for $\beta = 0$:

$$\lambda_{\max} = D(1 - \cos\Phi). \tag{4}$$

The shortest wavelength is achieved for $\alpha \approx \beta \approx \Phi/2$ and is limited only by the mirror reflectivities and the scattering by the diffraction grating near the zero order for a given angle of incidence.

A monochromatic probe beam is incident on a toroidal mirror TM intended for the formation of the probe beam of requisite shape on a sample under investigation. The sagittal and meridional torus radii are so selected that the torus constructs the image of the radiation source in the vertical plane and constructs the image of the exit slit S2 in the horizontal one. The angle of radiation incidence on the torus is equal to 1.5°. Since the angle of incidence is quite low and the mirror is not changed in going over from one spectral range to another, the torus is coated with gold with a average reflectivity of 80% (averaged over the entire working range).

The probe beam intensity is monitored with a detector-monitor MON placed between the exit slit and the torus. The detector is a secondary electron multiplier made up of two microchannel plates of shevron type. For a photocathode use is made of a metal mesh with a thin layer of CsI deposited on it. The presence of a detector-monitor permits to record the pulse-to-pulse variation of radiation intensity. The relation between the reflection (transmission) coefficient $R$ of an optical element under investigation and signals from the monitor ($I_{\mathrm{m}}$) and the detector ($I_{\mathrm{rd}}$), which records the reflected (transmitted) signal, is expressed as follows:

$$R = K\frac{I_{\mathrm{rd}}}{I_{\mathrm{m}}}, \tag{5}$$

where $K(\lambda) = I_{\mathrm{m}}(\lambda)/I_{0\mathrm{d}}(\lambda)$ is the spectral dependence of the monitor–detector signal ratio measured prior to the procedure of testing the optical element when the sample is withdrawn from the beam.

The probe beam reflected from the toroid is focused on the axis of the goniometer, which accommodates the sample under study. Since the majority of samples are curvilinear in surface shape and the their numerical aperture NA may range up to 0.5 for mirror diameters of up to 300–500 mm, the goniometer has seven degrees of freedom to provide positioning of any sample's point on the goniometer axis and alignment of the local axis with the beam axis. For the reflectometer we designed a goniometer whose prototype was described in Refs [1, 3]. The goniometer provides the following motions: vertical ($Z$) and horizontal ($X$) translations, rotation about axis $X$ ($\omega$ rotation) and rotation about axes $Z$ ($\varphi$ rotation) and $Y$ ($\theta$ rotation), as well as two degrees of freedom for the detector: $2\varphi$ and $2\theta$ rotations. The difference from the prototype is a larger (up to 500 mm) diameter of the samples which may be investigated with this goniometer. The main parameters of the optical reflectometer configuration are given below*, and the parameters of the motions provided by the goniometer are collected in Table 1.

Distances/mm
- Radiation source – S1 . . . . . 35
- S1–M1 . . . . . 1200
- M1–M2 . . . . . 170
- M2–S2 . . . . . 400
- S2–TM . . . . . 200
- TM–S . . . . . 800
- Radiation source–TM (with account for the path lengths between the mirrors and the diffraction grating) 2025

Slit widths/μm
- S1 . . . . . 100
- S2 . . . . . 33

Radii of curvature/mm
- M1 . . . . . 45858.00
- M2 . . . . . 15285.00
- TM (sagittal) . . . . . 12224.00
- TM (meridional) . . . . . 30.40

Limiting (measured) resolution in the middle of the range ($\lambda_{\mathrm{c}}/\Delta\lambda$)
- Grating, 900 lines mm$^{-1}$ . . . . . 556 (500)
- Grating, 400 lines mm$^{-1}$ . . . . . 500 (450)

**Table 1.** Main characteristics of the motions provided by the goniometer.

| Motion type | Motion range | Motion accuracy |
|---|---|---|
| $X$ coordinate/mm | 50 | 0.1 |
| $Z$ coordinate/mm | 250 | 0.1 |
| $\omega$ rotation/deg | 360 | 0.1 |
| $\varphi$ rotation/deg | 360 | 0.025 |
| $\theta$ rotation/deg | ±30 | 0.025 |
| $2\varphi$ rotation/deg | 360 | 0.025 |
| $2\theta$ rotation/deg | ±30 | 0.025 |

The intensity of radiation reflected from (or transmitted through) a sample under investigation is recorded with a detector D, which is similar to the detector-monitor but is different from it in the photocathode design: the photocathode is a polished stainless plate coated with a CsI film 100 nm in thickness.

The goniometer provides the main scanning modes of interest to X-ray optical scientists: $\varphi$-$2\varphi$, $Z$ and $X$ scanning for fixed angular positions of the sample and the detector, as well as $2\varphi$ and $2\theta$ detector scanning for a fixed sample position (measurement of scattering indicatrices).

The problem of intensity loss of the probe monochromatic beam due to additional reflections from the collimating mirrors was solved by applying two-layer Cr(10 nm)–C(5 nm)

* The lengths indicate the distances between the centres of the corresponding elements. The limiting spectral resolution was obtained by formula (3) with account for the widths of both slits.

coatings proposed and studied in Ref. [14]. The idea of these coatings is that the critical angle in the long-wavelength part of the working range is larger, and for the outer layer use can be made of a material with a lower atomic number (C in our case) and, accordingly, with a lower loss by absorption. The shorter-wavelength radiation passes through the upper layer and is reflected from the inner layer (Cr) with a higher atomic number. In comparison with heavy-metal coatings (gold, tungsten) traditionally employed for these purposes, the loss reduction may amount to 30% and over, which (in view of triple reflection) improves the spectrometer efficiency by nearly a factor of two.

For additional information about the parameters of optical elements, design principles and aberration minimisation of the spectrometer/monochromator, see Refs [12, 13].

## 3. Testing of reflectometer characteristics

The main reflectometer characteristics are the working wavelength range, intensity (dynamic range in intensity), spectral width (the spectral resolution of the spectrometer/monochromator), and the size of the probe beam on a sample under investigation. In the present series of experiments the polariser (see Fig. 1) was not used. The experiments were carried out with the use of two diffraction gratings made in the State Institute of Applied Optics (Kazan). One grating is a ruled echelette grating with a groove density of 900 lines $mm^{-1}$, the other is a holographic grating with line density of 400 lines $mm^{-1}$.

To improve the diffraction efficiency in the short-wavelength part of the working range, the echelette was subjected to ion beam polishing. As a result, its efficiency in the 4.47 nm region rose from 0.4% to 3% and from 5.2% to 13% at a wavelength of 8.21 nm. Depositing the Cr(10 nm)–C(5 nm) reflective coating improved the efficiency up to 11.2% and 18.4%, respectively [15].

According to the measurement data outlined in Ref. [16], the X-ray LPPS measures 100×150 μm at half-height of the intensity profile.

The size of the probe beam on a sample was measured at 500×400 μm using the knife technique. The beam dimensions were approximately four times greater than the design dimensions, which is supposedly due to the quality of the toroidal mirror. This beam size nevertheless meets the main requirements for virtually all X-ray optical applications of interest in the EUV and SXR ranges.

The working wavelength range, the spectral resolution, and the dynamic intensity range of the instrument are largely determined by the characteristics of diffraction gratings. In accordance with formula (4), for $\Phi = 12°$ (the angle is defined by the instrument design) the longest wavelength is $\lambda_{max1}$ = 24.3 nm for the first grating and $\lambda_{max2}$ = 54.6 nm for the second one. Since the emission spectrum of dense plasma is quasi-continuous, initially (to estimate the contribution of higher diffraction orders to the intensity of the probe beam) the diffraction efficiency of the gratings in different diffraction orders was studied with a reflectometer [3]. The experiments were performed in conditions corresponding to the operating mode of the Czerny–Turner spectrometer/monochromator: the detector was placed at an angle $\Phi = 12°$ relative to the incident beam and only the grating was rotated. Measurements were made at the following characteristic lines: C $K_\alpha$ ($\lambda$ = 4.47 nm), Mo $M_\xi$ ($\lambda$ = 6.44 nm), Zr $M_\xi$ ($\lambda$ = 8.21 nm), Be $K_\alpha$ ($\lambda$ = 11.40 nm), Si $L_\alpha$ ($\lambda$ = 13.55 nm), Al $L_\alpha$ ($\lambda$ = 17.14 nm), Mg $L_\alpha$ ($\lambda$ = 25.15 nm), and He II ($\lambda$ = 30.4 nm).

Figure 2 shows measurement data for the ruled (groove density: 900 lines $mm^{-1}$) and holographic (400 lines $mm^{-1}$) gratings. Plotted on the abscissa is the working wavelength in the spectrometer, plotted on the ordinate is the contribution of higher diffraction orders to the probe beam signal. The curve number corresponds to the order number.

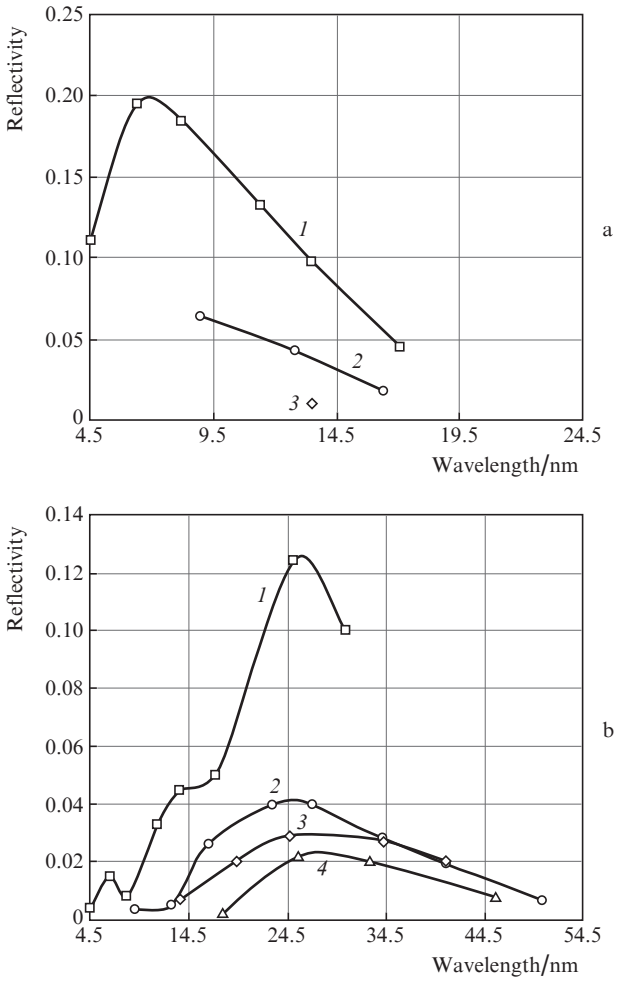


**Figure 2.** Contributions of diffraction orders to the probe signal intensity for (a) a ruled grating with a groove density of 900 lines $mm^{-1}$ and (b) a holographic grating with a line density of 400 lines $mm^{-1}$ in relation to the wavelength. The curve number corresponds to the number of diffraction order.

As is clear from Fig. 2, in the performance of precision measurements it is necessary to take into account the contribution of higher diffraction orders to the probe beam intensity, otherwise large errors would be expected to occur in the measurements.

The calculated contributions of the orders to the probe beam intensity expressed in percents of the first-order intensity are collected in Table 2. In the calculations it was assumed that the spectral intensity function has the shape of a plateau, i.e. is independent of the wavelength. Also, it was taken into account that the wavelength interval $\Delta\lambda_m$ at the monochromator output is inversely proportional to the order number ($\Delta\lambda_m \sim 1/m$) due to dispersion.

Figure 3a shows a typical LPPS spectrum of a stainless steel target (without accounting for higher orders) measured with the ruled diffraction grating (900 lines $mm^{-1}$). Each point

**Table 2.** Diffraction order contributions to the probe signal intensity (in percentage of the first-order intensity).

| Order number, $m$ | Efficiency relative to 1st order (%) | |
|---|---|---|
| | Ruled grating | Holographic grating |
| 1 | 100 | 100 |
| 2 | 18.9 | 16.5 |
| 3 | 3.4 | 8.4 |
| 4 | – | 4.8 |

of the spectral curve is an average over 30 laser pulses. In accordance with formula (4), the longest wavelength is equal to 24 nm. The highest intensity of the probe beam falls on the 10–13 nm spectral range. The radiation intensity recorded in the wavelength range below 5 nm is due to the radiation scattering by the grating. This wavelength is the short-wavelength boundary of the working range.

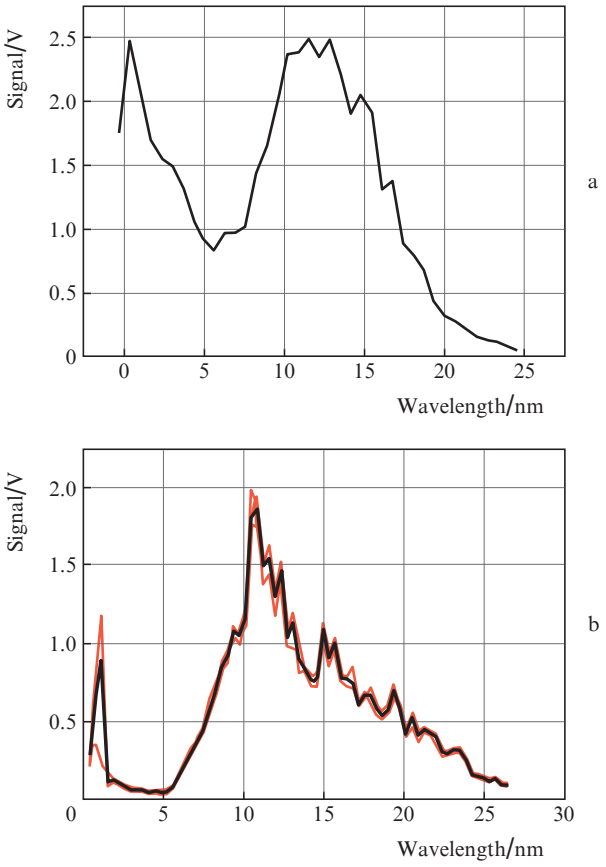


**Figure 3.** Recorded spectra of the laser-plasma source with a stainless steel target: (a) ruled grating, (b) holographic grating.

Figure 3b depicts the spectrum recorded with the holographic grating (400 lines $mm^{-1}$). Plotted in Fig. 3b are five sequentially recorded curves (thin solid lines) and the spectral dependence of probe beam intensity averaged over these curves (thick solid line). Each point of the spectral curves is an average over 30 laser pulses, and so every point of the averaged curve was obtained for 150 pulses. The longest radiation wavelength is equal to 52 nm. The highest intensity falls on the 20–25 nm domain, which corresponds to the peak of diffraction efficiency of the grating and supposedly to the peak of the source intensity. The presence of several curves in the drawing, which correspond to a series of sequential measurements, is illustration that, first, the shot-to-shot reproducibility of the spectral source characteristics is rather high and, second, the spikes observed in the curves are due not signal intensity fluctuations but correspond to real spectral features (the spectral lines of differently charged ions and different chemical elements).

As follows from the shapes of the spectral curves, the problem of higher-order contribution to the probe beam intensity is of current importance. For instance, in view of the grating efficiency and the shape of the spectrum (Table 1 and Fig. 3b) the 2nd-order contribution to the probe beam intensity in the 40-nm domain will range up to almost 40%. We believe that the solution of this problem lies with the use of filters. For instance, for measurements in the 17-to-34 nm domain it would suffice to employ an Al filter of thickness 200 nm (Fig. 4). The use of this filter with a transmittance of 60%–70% permits suppressing the second order by more than a factor of 100 (wavelengths: 8.5–17 nm) and the third order by factors of 50–500 (wavelengths: 5.6–11.3 nm) throughout the working range (indicated with dashed arrows). A similar behaviour is exhibited by Mg-based filters in the 27–54 nm range. The technologies of free-standing multilayer filter fabrication developed in IPM RAS permit covering with confidence the entire working wavelength range [17, 18].

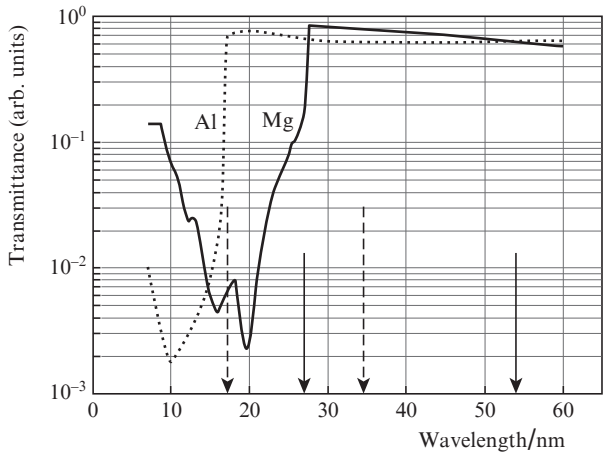


**Figure 4.** Spectral dependences of the transmission coefficients of Al and Mg filters of thickness 0.2 Mm. The working reflectometer ranges with Al and Mg filters are indicated by dashed solid arrows.

Since the spectral resolution of a spectrometer/monochromator is most often determined by alignment inaccuracies and the geometrical aberrations of the optical system as a whole, the form of the zero-order spectrum characterises the resolution of the instrument to the largest extent. The efficiency and reliability of this simple technique of measuring the resolution was demonstrated in Ref. [19] by the example of studies of the narrow spectral lines Al $K_\alpha$ (wavelength: 0.834 nm; linewidth: below 0.001 nm), Mg $K_\alpha$ (0.989 nm; linewidth: 0.001 nm), and Fe $L_\alpha$ (1.76 nm; linewidth: 0.003 nm). By analogy with Refs [4, 5], the resolution was also determined from the steepness of the transmission coefficient in the vicinity of the absorption edges of filter materials. The results of measurements by the two techniques are in satisfactory agreement. Figure 5 shows the measured spectral dependences of zero-order probe-beam intensity for the ruled and holo-

graphic gratings. With reference to Fig. 5, the spectral resolution at half-height intensity of the signals was measured at 0.030 nm for the ruled grating and 0.067 nm for the holographic one. This corresponds to a spectral resolving power $\lambda/\Delta\lambda \approx 500$ at the central working-range wavelength $\lambda_c = 15$ nm and to $\lambda/\Delta\lambda \approx 450$ at $\lambda_c = 30$ nm, respectively. This is, first, slightly worse than the calculated resolving power (556 and 500, respectively, see above) and, second, quite sufficient for the solution of the majority of X-ray optical problems.

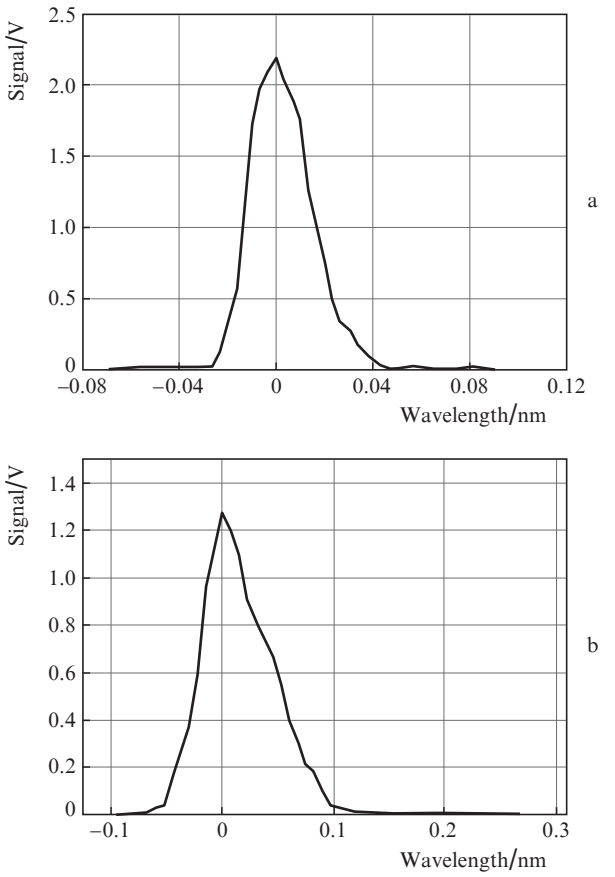


**Figure 5.** Spectral dependences of the zero-order probe-beam intensity for (a) the ruled and (b) holographic diffraction gratings. Negative wavelength values correspond to the opposite order.

The number of photons in the probe beam was estimated at a wavelength of 13.5 nm using an absolute-calibrated SPD UV detector with a multilayer Zr/Al filter coating deposited on its surface (the calibration detector curve was given in Ref. [20]). The spectral power density in this region amounted to about $10^8$ photons $s^{-1}$ 0.1 $nm^{-1}$, which is approximately 1.5 times lower than expected (see Ref. [13]) and is comparable with the data for laboratory reflectometers [4, 5, 7].

In experiments performed with the use of microchannel plate detectors the dynamic range of the instrument in probe beam intensity was higher than $10^3$ throughout the working wavelength range.

## 4. Examples of reflectometer applications to the study of X-ray optical elements

At present the reflectometer is used to measure the reflection and transmission coefficients of the elements of multilayer optics. Figure 6a shows the angular dependences of the reflectivity of a Mo/Be multilayer mirror (150 5.93-nm thick periods) measured at a wavelength of 11.38 nm. One can see from Fig. 6a that the peak reflectivity and the resonance wavelengths coincide to within approximately ±1.5%. The reader's attention is drawn to the fact that the subsidiary maxima observed to the left of the Bragg peak on the curve measured on a synchrotron are hardly resolved with the laboratory instrument. Nevertheless, the laboratory curve describes their average value quite well. This circumstance will be taken into account in the reconstruction of the structural parameters of multilayer mirrors from the measured angular dependences of reflection coefficients in the soft and hard X-ray ranges.

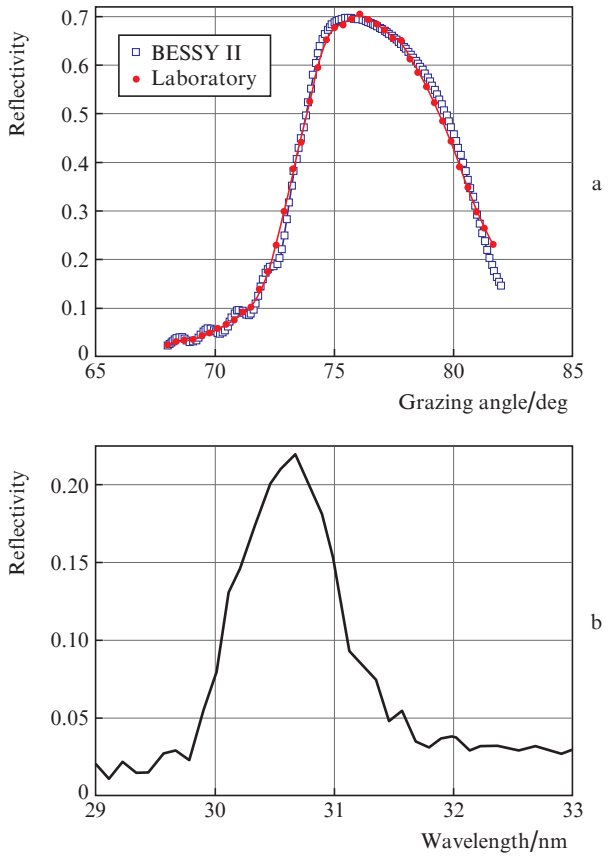


**Figure 6.** (a) Angular dependences of the reflectivity of a Mo/Be multilayer mirror (150 5.93-nm thick periods) measured at a wavelength of 11.38 nm: the curve labelled Laboratory corresponds to the measurements made with the instrument under description (each point on the laboratory curve was obtained by averaging over 30 laser pulses), and the curve labelled BESSY II was measured on the BESSY II synchrotron; (b) spectral dependence of the reflectivity of an Si/Mg mirror measured with the reflectometer reported in this work.

Figures 6b and 7 illustrate the new possibilities which emerged in connection with the development of the instrument. Plotted in Fig. 6b is the measured spectral dependence of the reflection coefficient of the Si/Mg multilayer mirror, which is under development for the solar research at a wavelength of 30.4 nm (He II) [21]. These measurements at the He II line were earlier made using a low-pressure gas discharge. Since the line is narrow (several orders of magnitude narrower than the bandwidth of the multilayer mirror), the resolving power of the mirrors in this spectral domain can be

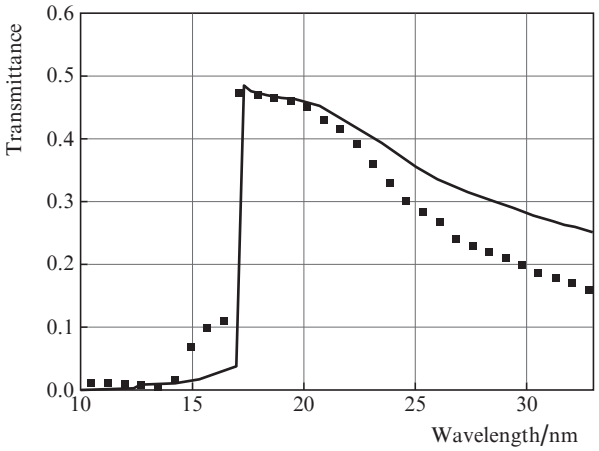


**Figure 7.** Spectral dependence of the transmission coefficient of a Al/Si multilayer filter (thickness of Al, 2.9 nm; thickness of silicon, 2.1 nm; number of periods, 55 + one Si layer). Solid line is the simulation, points show the measurement data.

estimated using the well-known formula which relates the spectral resolution to the width of the angular dependence of the reflectivity at a fixed wavelength. This approach works quite well in the short-wavelength domain, where the dispersion of optical constants within the multilayer mirror bandwidth is low, but works unsatisfactorily in the EUV domain, where the mirrors have a broad bandwidth in which optical material constants exhibit appreciable variations. Owing to the presence of a broadband radiation source (LPPS) our reported reflectometer permits carrying out these experiments.

The reflectometer makes it possible to study the spectral dependences of filter transmittances. This dependence for a free-standing Al/Si multilayer structure intended for the suppression of long-wavelength radiation (an absorption filter) is plotted in Fig. 7. With reference to Fig. 7, while the calculated and experimental data coincide immediately near the absorption edge, with increasing wavelength they show a disagreement, which is likely to arise from film oxidation. This is attested by the existence of transmission behind the absorption edge, which is indication of the presence of an oxide layer on the film surface.

## 5. Conclusions

Our work describes in detail a laboratory reflectometer developed at the IPM RAS on the basis of a laser-plasma source of SXR and EUV radiation and a Czerny–Turner spectrometer/monochromator. The reflectometer is intended for precision measurements of the spectral characteristics of X-ray optical elements in a wavelength range of 5–50 nm. The working range of the instrument may be extended both to the long-wavelength side and to the short-wavelength side by employing diffraction gratings with a longer or shorter period. In particular, a diffraction grating with a line density of 300 $mm^{-1}$ will permit operation up to a wavelength of 73 nm, with spectrometer selectivity $\lambda/\Delta\lambda \approx 500$ in this case. In the future we plan to improve spectral resolution by replacing spherical collimator mirrors with aspheric ones, as shown in Ref. [13].

At present, the short-wavelength boundary (5 nm) of the instrument is limited by the strong radiation scattering from the ruled diffraction grating. We investigated several diffraction gratings, including those with different line densities. Although they exhibited a fairly good first-order diffraction efficiency, the highest monochromatic radiation-to-background intensity ration did not exceed a figure of 10 in the short-wavelength domain. Holographic gratings optimised for this wavelength range will be produced for the solution of this problem.

Despite the limitation in one technical characteristic, namely in breadth of the working wavelength range that maintains a high spectral resolution, the proposed reflectometer outperforms the closest analogues in the world [4, 5, 7]. An advantage of the reflectometer over the instruments employing X-ray tubes and gas-discharge radiation sources [1–3] is a stronger signal and a broad emission spectrum of the laser-plasma source.

Our instrument permits studying mirrors with an arbitrary surface shape up to 500 mm in diameter. Owing to a high intensity of the probe beam, in the future it will be possible to employ polarising and phase-shifting free-standing multilayer structures, which will significantly broaden the reflectometer capabilities [22].

***Acknowledgements.*** This work was supported by the Presidium of the Russian Academy of Sciences (Programme 'Extreme laser radiation: physics and fundamental applications') and by the RSF–DFG Grant No. 16-42-01034 with respect to the development of techniques for measuring X-ray multilayer optical elements.

## References

1. Andreev S.S., Akhsakhalyan A.D., Bibishkin M.S., et al. *Central Europ. J. Phys.*, **1**, 191 (2003).
2. Chkhalo N.I., Fedorchenko M.V., Kovalenko N.V., Kruglyakov E.P., et al. *Nucl. Instrum. Meth. Phys. Res. A*, **359**, 121 (1995).
3. Bibishkin M.S., Chekhonadskih D.P., Chkhalo N.I., et al. *Proc. SPIE*, **5401**, 8 (2004).
4. Gullikson E.M., Underwood J.H., Batson P.C., Nikitin V. *J. X-Ray Sci. Technol.*, **3**, 283 (1992).
5. Loyen L., Bottger T., Braun S., et al. *Proc. SPIE*, **5038**, 12 (2003).
6. Hettrick M.C., Underwood J.H. *AIP Conf. Proc.*, **147**, 245 (1986).
7. Miyake A., Miyachi T., Amemiya M., et al. *Proc. SPIE*, **5037**, 647 (2003).
8. Vishnyakov E.A., Kolesnikov A.O., Ragozin E.N., Shatokhin A.N. *Nanofizika i Nanoelektonika* (Nanophysics and Nanoelectronics) (Proc. XX Intern. Symp., 14–18 March 2016, N. Novgorod) **2**, 368 (2016); http://nanosymp.ru/UserFiles/Symp/2016_v1.pdf.
9. Chkhalo N.I., Salashchenko N.N. *AIP Advances*, **3**, 082130 (2013).
10. Barysheva M.M., Pestov A.E., Salashchenko N.N., et al. *Phys. Usp.*, **55** (7), 681 (2012) [*Usp. Fiz. Nauk*, **182** (7), 727 (2012)].
11. Artioukov I.A., Vinogradov A.V. *Opt. Lett.*, **20**, 2451 (1995).
12. Tondello G., Zanini F. *Rev. Sci. Instrum.*, **60**, 2116 (1989).
13. Dogadin V.O., Zuev S.U., Salashchenko N.N., Chkhalo N.I., Shcherbakov A.V. *Poverkhnost'. Rentgenovskie, Sinkhrotronnye i Neitronnye Issledovaniya*, **7**, 77 (2015).
14. Chkhalo N.I., Gaikovich P.K., Salashchenko N.N., Yunina P.A., Zuev S.Yu. *Thin Solid Films*, **598**, 156 (2016).
15. Zorina M.V., Zuev S.U., Mikhailenko M.S., Pestov A.E., et al. *Pis'ma Zh. Tekh. Fiz.*, **42**, 34 (2016).
16. Nechai A.N., Pestov A.E., Polkovnikov V.N., Salashchenko N.N., et al. *Quantum Electron.*, **46**, 347 (2016) [*Kvantovaya Elektron.*, **46**, 347 (2016)].
17. Chkhalo N.I., Drozdov M.N., Kluenkov E.B., Lopatin A.Ya., et al. *J. Micro/Nanolith. MEMS MOEMS*, **11**, 021115 (2012).
18. Chkhalo N.I., Drozdov M.N., Kluenkov E.B., Kuzin S.V., et al. *Appl. Opt.*, **55**, 4683 (2016).
19. Chkhalo N.I. *Mnogosloinye rentgenovskie zerkala. Diagnostika i primeneniya* (X-ray Multilayer Mirrors. Diagnostics and Applications) (LAP LAMBERT Acad. Publ., 2011).

20. Aruev P.N., Barysheva M.M., Ber B.Ya., Zabrodskaya N.V., Zabrodskii V.V., Lopatin A.Ya., Pestov A.E., Petrenko M.V., Polkovnikov V.N., Salashchenko N.N., Sukhanov V.L., Chkhalo N.I. *Quantum Electron.*, **42**, 943 (2012) [*Kvantovaya Elektron*., **42**, 943 (2012)].
21. Bogachev S.A., Chkhalo N.I., Kuzin S.V., Pariev D.E., et al. *Appl. Opt.*, **55**, 2126 (2016).
22. Andreev S.S., Bibishkin M.S., Chkhalo N.I., et al. *Nucl. Instrum. Meth. Phys. Res. A*, **543**, 340 (2005).